Quantification of Conventional and Non-Conventional Charge-Assisted Hydrogen Bonds in the Condensed and Gas Phases

ARTICLE *in* JOURNAL OF PHYSICAL CHEMISTRY LETTERS · OCTOBER 2015

Impact Factor: 7.46 · DOI: 10.1021/acs.jpclett.5b02175

8 AUTHORS, INCLUDING:

Sergey A Katsyuba

Russian Academy of Sciences

105 PUBLICATIONS **882** CITATIONS

SEE PROFILE

Mikhail V Vener

Mendeleev Russian University of Chemical T…

69 PUBLICATIONS **1,189** CITATIONS

SEE PROFILE

Elena E. Zvereva

Russian Academy of Sciences

37 PUBLICATIONS **606** CITATIONS

SEE PROFILE

Rosario Scopelliti

École Polytechnique Fédérale de Lausanne

427 PUBLICATIONS **10,094** CITATIONS

SEE PROFILE

THE JOURNAL OF PHYSICAL CHEMISTRY Letters

Letter

pubs.acs.org/JPCL

Quantification of Conventional and Nonconventional Charge-Assisted Hydrogen Bonds in the Condensed and Gas Phases

Sergey A. Katsyuba,*[,†] Mikhail V. Vener,[‡] Elena E. Zvereva,[†,§] Zhaofu Fei,[∥] Rosario Scopelliti,[∥] Jan Gerit Brandenburg,[⊥] Sviatlana Siankevich,[∥] and Paul J. Dyson*[,∥]

[†]A. E. Arbuzov Institute of Organic and Physical Chemistry, Kazan Scientific Centre of the Russian Academy of Sciences, Arbuzov Street 8, 420088 Kazan, Russia

[‡]Department of Quantum Chemistry, Mendeleev University of Chemical Technology, Miusskaya Square 9, 125047 Moscow, Russia

[§]Institut de Nanosciences et Cryogénie, SP2M/L_sim, CEA, 17 Rue des Martyrs, 38054 Grenoble, France

[∥]Institut des Sciences et Ingénierie Chimiques, Ecole Polytechnique Fédérale de Lausanne (EPFL) EPFL − BCH, CH-1015 Lausanne, Switzerland

[⊥]Mulliken Center for Theoretical Chemistry, Institut für Physikalische und Theoretische Chemie der Universität Bonn, Beringstrasse 4, 53115 Bonn, Germany

Supporting Information

ABSTRACT: Charge-assisted hydrogen bonds (CAHBs) play critical roles in many systems from biology through to materials. In none of these areas has the role and function of CAHBs been explored satisfactorily because of the lack of data on the energy of CAHBs in the condensed phases. We have, for the first time, quantified three types of CAHBs in both the condensed and gas phases for 1-(2′-hydroxylethyl)-3-methylimidazolium acetate ([C_2OHmim][OAc]). The energy of conventional OH···[OAc]$^-$ CAHBs is ∼10 kcal·mol^{-1}, whereas nonconventional C(sp2)H···[OAc]$^-$ and C(sp3)H···[OAc]$^-$ CAHBs are weaker by ∼5−7 kcal·mol^{-1}. In the gas phase, the strength of the nonconventional CAHBs is doubled, whereas the conventional CAHBs are strengthened by <20%. The influence of cooperativity effects on the ability of the [OAc]$^-$ anion to deprotonate the imidazolium cation is evaluated. The ability to quantify CAHBs in the condensed phase on the basis of easier accessible gas-phase estimates is highlighted.

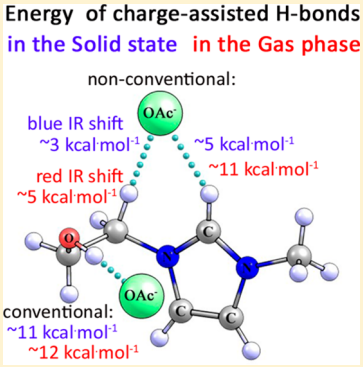

The strengthening of "conventional" XH···A (where X = O, N, or another very electronegative atom) and "nonconventional" CH···A hydrogen bonds (H-bonds) that occurs when either XH or A subunits (or both) are electrically charged[1−11] is an essential element for molecular recognition in a vast array of chemical and biological processes.[12−24] Consequently, quantifiable information on this phenomenon is regarded as essential for rational design of selective ligands, organocatalysts, drugs, and pesticides. Quantum chemical computations and gas-phase experiments have provided quantitative assessments of such charge-assisted H-bonds (CAHBs) in the gas phase, but their strength in the condensed phase has been investigated surprisingly little until now. It is well documented that in crystals, neat liquids, or in solutions where solvents participate in H-bonding with solutes, the presence of multiple H-bonds should influence their strengths relative to the case of the gas phase. Nevertheless, systematic studies of nonconventional CAHBs in the condensed phase have not been performed, and hence, CAHBs have not been quantified in the majority of systems of practical interest.

Among the condensed-phase systems, crystals represent a special, unique case. The geometrical, spectral, and electron density parameters of H-bonds in the condensed state of matter are simultaneously provided. Moreover, for crystals where density functional theory computations with periodic boundary conditions (solid-state DFT) are applicable, it is possible to analyze quantum chemically cooperative H-bonds in chemically relevant condensed-phase species. In particular, expressions that link the energy of H-bonds (E_{HB}) with the local electronic energy density (see below)[25,26] were proposed and successfully applied for E_{HB} estimation of the N−H···Cl$^-$ CAHB in crystals.[27]

Recently, we obtained the first quantitative estimates of the energy of both conventional and nonconventional intermolecular CAHBs in a crystal.[28] For this purpose, the solid-state electron density map of crystalline [C_2OHmim][PF_6] (Chart 1) was analyzed and combined with spectroscopic indicators of H-bond formation such as the red shift of the XH stretching vibrational frequency (νXH) and increase in IR intensity.[29,30] The estimates of the H-bond strength obtained with various empirical approaches were in excellent agreement with each other. E_{HB} for nonconventional CAHB C2H$^+$···[PF_6]$^-$ amounted to ∼2.8−3.1 kcal·mol^{-1}, whereas the conventional

Received: September 30, 2015
Accepted: October 23, 2015

DOI: 10.1021/acs.jpclett.5b02175
J. Phys. Chem. Lett. 2015, 6, 4431−4436

Chart 1. Atom Numbering Scheme for the 1-(2′-Hydroxylethyl)-3-methylimidazolium $[C_2OHmim]^+$ (a), 1-Butyl-3-methylimidazolium $[C_4mim]^+$ (b) Cations, and $[PF_6]^-$ (c) and $[OAc]^-$ (d) Anions

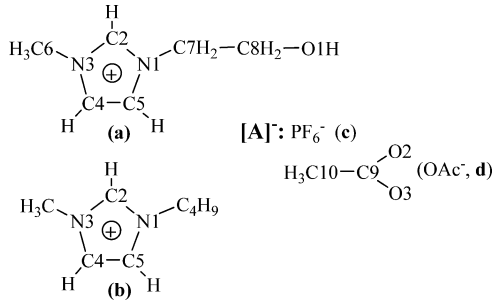

CAHB OH···$[PF_6]^-$ was found to be only slightly stronger (~3.4−3.8 kcal·mol^{-1}).

The reliability of the above-mentioned empirical correlations (eqs 1−3) in the case of crystalline $[C_2OHmim][PF_6]$ suggests that they are applicable also to analysis of H-bonding between the $[C_2OHmim]^+$ cation and the acetate anion $[OAc]^-$ in the solid state. In comparison with $[PF_6]^-$, one of the weakest H-bond acceptors, such a strongly basic anion as $[OAc]^-$ represents another extreme, and some specific effects could be anticipated for the $[C_2OHmim][OAc]$ system in comparison to $[C_2OHmim][PF_6]$. In particular, as will be shown herein, the $[OAc]^-$ anion forms nonconventional CAHBs with the protons of the imidazolium ring and with the protons of alkyl moieties of the cation. The strength of both conventional OH···$[OAc]^-$ and nonconventional CH···$[OAc]^-$ CAHBs has been evaluated and compared with the energies of OH···$[A]^-$ and CH···$[A]^-$ bonds with anions $[A]^-$ of various H-bond basicity, both cooperative and isolated. On these grounds, cooperativity effects were quantified.

Intermolecular H-bonds in gas-phase systems may be studied using energy decomposition schemes,[31,32] natural bond orbital,[33] and Bader analysis.[34] The applicability of the former two approaches to the identification and quantitative description of H-bonds in crystals is not straightforward, and the most substantial evidence for H-bonds in molecular crystals comes from the Bader analysis of the electronic density.[35,36] It has been suggested that Bader analysis should be used with caution for evaluation of the CAHB strength in the crystalline state.[34] To avoid possible ambiguity, two different sets of the computed properties were used in the present study for evaluation of the CAHB energy/enthalpy: (i) the electron density features at the H-bond critical point[25,26] and (ii) the spectroscopic features of the stretching vibrations of the XH group involved in CAHB formation.[29,30]

Spectroscopic indicators of H-bond formation such as red shifts of XH stretching vibrational frequencies (νXH) and increases in IR intensities[29,30] were used to evaluate the enthalpies ($-\Delta H_{HB}$) of intermolecular H-bonds in 1:1 H-bonded complexes in liquid phases (solutions)

$$-\Delta H_{HB}\ [\text{kcal·mol}^{-1}] = 0.29\Delta I^{1/2}\ [\text{kcal·mol}^{-1}] \quad (1)$$

where $\Delta I^{1/2} = I^{1/2} - I_0^{1/2}$ and I is the IR intensity for the localized, uncoupled stretching vibration (νXH) of the X−H group (X = O and C) participating in the H-bond compared to the noninteracting group (I_0)

$$-\Delta H_{HB}\ [\text{kcal·mol}^{-1}] = 0.33(\Delta\nu\ [\text{cm}^{-1}] - 40)^{1/2} \quad (2)$$

where $\Delta\nu = \nu XH_{free} - \nu XH_{bonded}$ represents the red-shift value of the νXH frequency caused by the formation of the H-bond with the XH group being the proton donor. Equations 1 and 2 were suggested for evaluation of $-\Delta H_{HB}$ for acid−base complexes in the liquid state.[29] It was later shown that these equations can be used to estimate the energy of the intermolecular H-bonds in crystals.[37−39] Applicability limits of eq 1 are discussed elsewhere.[37]

In crystals with X−H···O H-bonds (X = O, N, C), E_{HB} can be estimated using the local electronic kinetic energy density, G_b, at the H···O bond critical point in electron density[26]

$$E_{HB}\ [\text{kcal·mol}^{-1}] = 269G_b\ [\text{atomic units}] \quad (3)$$

Equation 3 enables the E_{HB} values to be evaluated using the experimental (precise X-ray diffraction data)[38] or theoretical periodic electron densities. The relevance of this expression for crystals with intermolecular H-bonds of different type and strength has been recently demonstrated.[37,38] The structure of $[C_2OHmim][OAc]$ was determined by single-crystal X-ray diffraction (Figure 1; Figure 1S, Supporting Information). The

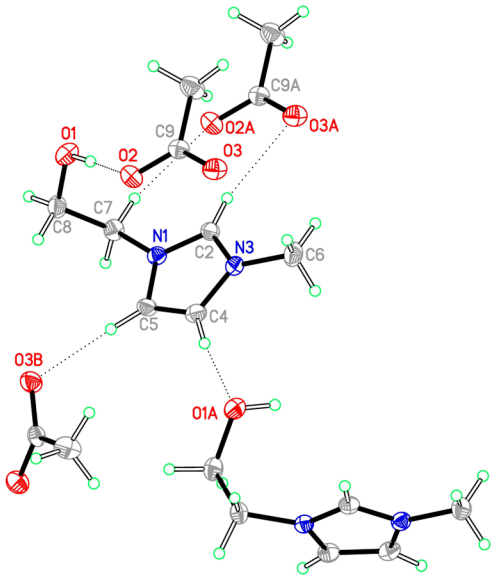

Figure 1. ORTEP plot of the crystal structure of $[C_2OHmim][OAc]$ showing the main interactions of the $[C_2OHmim]^+$ cation with the immediate surrounding environment (by dashed lines). Letters A and B, shown in the labels, indicate symmetry-related atoms.

packing motif in the crystal is characterized by multiple short contacts between the counterions. Each cation forms short contacts with another cation and three anions (Figure 1) via all C(sp2)H moieties of the imidazolium ring and the C(sp3)H moiety of the methylene group adjacent to the nitrogen atom. The experimental values of the atomic positions of the $[C_2OHmim][OAc]$ crystal were used as the starting point in the solid-state DFT computations, which took into account nonlocal London dispersion interactions within the framework of the D3 correction scheme (see the Supporting Information for details). The computed X···O distances (Table 2S) and IR spectrum (Figure 2S, Table 3S) of the crystal are in good agreement with the experimental ones. The H-bonds in the crystal are characterized by R(X···O) distances of <3.3 Å, X−H···O angles > 150°, electron densities at critical points, ρ_b, of ~0.02−0.05 au, $\nabla^2\rho_b > 0$, and energies E_{HB} of ~4−10 kcal·mol^{-1} (Table 1 and Table 2S).

DOI: 10.1021/acs.jpclett.5b02175
J. Phys. Chem. Lett. 2015, 6, 4431−4436

Table 1. Values of the Computed X···O Distances R(X···O) of the X−H···O Units (Where X = O or C) in the [C_2OHmim][OAc] along with the H-Bond Energy, E_{HB} and Enthalpy, $-\Delta H_{HB}$, and Shifts, $\Delta\nu$XH, Relative to the Isolated [C_2OHmim]$^+$ Cation[40] in the Solid State and in the Gas (in Parentheses)

	C2H···O3[a]	C4H···O1[a]	C5H···O3[a]	C7H···O2[a]	O1−H···O2[a]
R(X···O), Å	3.19 (2.76)	3.25 (2.74)	3.10 (2.78)	3.19 (3.02)	2.64 (2.57)
E_{HB},[b] kcal·mol^{-1}	3.6 (11.0)	3.4 (11.0)	4.6 (10.3)	3.6 (5.1)	10.1 (13.0)
$-\Delta H_{HB}$,[c] kcal·mol^{-1}	4.9 (10.4)	3.4 (10.2)	5.4 (10.8)	1.7 (3.3)	9.6 (10.2)/8.1 (10.0)[d]
$\Delta\nu$XH, cm^{-1}	−154 (−770)	−94 (−804)	−126 (−793)	+36 (−87)	−645 (−959)

[a]The original numeration of atoms taken from Figure 1. [b]Evaluated using eq 3. [c]Evaluated using eq 1. [d]Evaluated using eq 2.

Table 2. Experimental Wavenumbers of the νOH and νC(sp2)H Bands in the Spectra of [C_2OHmim][A] Salts;[28] Red Shifts, $\Delta\nu$OH, Relative to the Isolated [C_2OHmim]$^+$ Cation;[40] and Enthalpies, $-\Delta H_{HB}$, of OH···[A]$^-$ H-Bonds[a]

anion [A]$^-$	νOH, cm^{-1}	$\Delta\nu$OH, cm^{-1}	$-\Delta H_{HB}$, kcal·mol^{-1}	νC(sp2)H, cm^{-1}
[PF_6]$^-$	3598 (3618[b])	100 (69[c])	2.3 (1.9)	3126, 3174
[BF_4]$^-$	3550 (3571[d])	148 (118[c])	3.3 (2.9)	3123, 3166
[$(CF_3SO_2)_2N$]$^-$	3544	154	3.4	3123/3107, 3161
[CF_3SO_3]$^-$	3451 (3500[e])	247 (187[c])	4.7 (4.0)	3119/3098, 3158
[CF_3CO_2]$^-$	3292	406	6.2	3099, 3153
[OAc]$^-$	3005	693	8.1	3093, 3146

[a]The corresponding data for MeOH···[A]$^-$ H-bonds are given in parentheses. [b]Reported for methanol solution in [C_4mim][PF_6] ionic liquid[46] and a MeOH/[Et_4N][PF_6] 1:1 mixture in the CH_2Cl_2 solution.[47] [c]Estimated relative to the experimental νOH frequency of MeOH in the gas phase (3687 cm^{-1}).[47] [d]Reported for a MeOH/[Et_4N][BF_4] 1:1 mixture in the CH_2Cl_2 solution.[47] [e]Reported for a MeOH/[Et_4N][OTf] 1:1 mixture in the CH_2Cl_2 solution.[47]

Nonconventional H-bonds involving CH protons are often difficult to identify, that is, to distinguish from van der Waals short contacts.[41−44] In crystalline [C_2OHmim][OAc], CAHBs formed by both the C(sp2)H and C(sp3)H protons are quite pronounced, simultaneously satisfying geometrical, IR spectroscopic, and electron topology criteria. It should be noted that C(sp3)H···[OAc]$^-$ nonconventional CAHB, involving the participation of the C7H group of the methylene moiety at the N1 atom, is blue-shifting, in contrast to C(sp2)H···O red-shifting H-bonds. As shown elsewhere,[45] a field-dominated blue-shifting may occur if the isolated H-bond donor with a negative dipole moment derivative, $d\mu_0/dr_{XH}$, interacts with anionic charge at large intermolecular distances. Our computations of isotope-isolated samples of the [C_2OHmim]-[OAc] crystal show that $d\mu_0/dr_{C7H}$ is positive. It is known that in general, the blue shift for νCH is a result of a subtle balance of opposing factors, for example, hyperconjugation and rehybridization.[33] In our case, the forces causing the blue shift for the C7H dominate over the other forces owing to multiple secondary interactions functioning in the crystal. This is clearly seen from a comparison of $\Delta\nu$C7H values for the crystal and the gas phase (Table 1), which will be discussed below.

The enthalpies ($-\Delta H_{HB}$) of the H-bonds in the crystal were estimated using eq 1 and, in the case of the O−H···O bond, applying eqs 1 and 2. For this purpose, vibrational frequencies νXH and their IR intensities were calculated for isotope-isolated samples of the [C_2OHmim][OAc] crystal (ν, I) and the [C_2OHmim]$^+$ cation (ν_0, I_0).[28] The estimated $-\Delta H_{HB}$ values are in reasonable agreement with the corresponding E_{HB} values (Table 1), considering that these quantities are connected with each other by the relation $E_{HB} = -\Delta H_{HB} + 3RT/2$. Thus, at room temperature, about 1 kcal·mol^{-1} should be added to the $-\Delta H_{HB}$ values in Table 1 to produce the E_{HB} values.

Good quality of the $-\Delta H_{HB}$(OH···A$^-$) estimates obtained with the use of eq 2 for A$^-$ = [OAc] and [PF_6][28] and well-known reliability of this empirical relationship for quantification of H-bonds formed by hydroxyl groups allow the strengths of OH···A$^-$ H-bonds between [C_2OHmim]$^+$ cation and various anions [A]$^-$ in solid or liquid salts to be compared with similar H-bonds formed by neutral molecules with the same anions in solutions (Table 2).

The data in Table 2 demonstrate that the H-bond parameters for neutral methanol closely match the corresponding values for the similar H-bonds formed by the [C_2OHmim]$^+$ cation in ionic liquids. Thus, the positive charge on the H-bond donor only slightly strengthens, by ∼20%, the conventional OH···[A]$^-$ CAHBs in the condensed phase.

Analysis of the frequencies collated in Table 2 suggests that the enthalpy, and hence the energy, of the nonconventional C(sp2)H···[A]$^-$ H-bonds follows the order found for the experimentally determined red shifts of the νC(sp2)H: [PF_6] < [BF_4] < [$(CF_3SO_2)_2N$] < [CF_3SO_3] < [CF_3CO_2] < [OAc]. The energy of the C(sp2)H···[PF_6]$^-$ H-bond (E_{HB}) is ∼3 kcal·mol^{-1} in solid [C_2OHmim][PF_6],[28] whereas for [C_2OHmim]-[OAc], E_{HB} is ∼4−6 kcal·mol^{-1} (Table 1). Thus, the strengths of H-bonds formed in the condensed phases by C(sp2)H moieties of the [C_2OHmim]$^+$ cations combined with a variety of different anions fall in a rather narrow range, that is, 3−6 kcal·mol^{-1}.

To quantify the strength of the CAHBs in the gas phase, we optimized quantum chemically various structures of possible isolated [C_2OHmim][OAc] ion pairs (Figure 3S) and estimated the energies/enthalpies of their H-bonds with the use of eqs 1−3. The complete set of structural, spectroscopic, electron topology, and energetic parameters of the strongest CAHBs between the counterions in the gas phase can be found in Table 4S. Some representative structures of isolated ion pairs are shown in Figure 2. They are stabilized by both conventional OH···[OAc]$^-$ and nonconventional C(sp2)H···[OAc]$^-$ and C(sp3)H···[OAc]$^-$ CAHBs. E_{HB}'s of conventional OH···[OAc]$^-$ H-bonds in the ion pairs (∼11−13 kcal·mol^{-1}) and in the bulk sample (∼9−11 kcal·mol^{-1}) almost coincide. In

DOI: 10.1021/acs.jpclett.5b02175
J. Phys. Chem. Lett. 2015, 6, 4431−4436

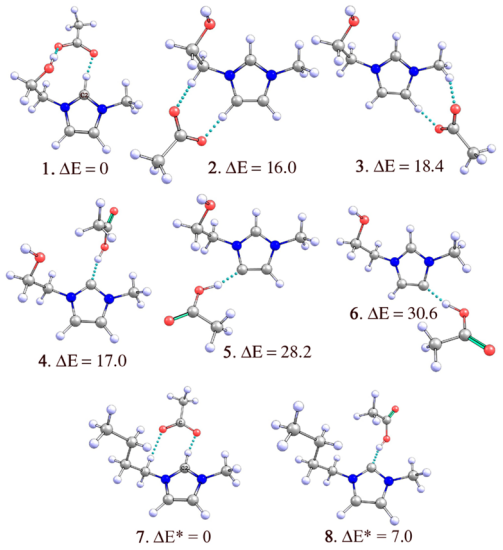

Figure 2. Optimized structures of ion pairs for $[C_2OHmim][OAc]$ (**1**–**6**) and $[C_4mim][OAc]$ (**7**, **8**) and their relative electronic energies (ΔE, kcal·mol^{-1}). Short contacts between O (or C) and H atoms are indicated with dotted lines.

contrast, the strength of the nonconventional C(sp2)H···$[OAc]^-$ H-bonds in the gas phase increases dramatically relative to that in the solid state (Table 1); C(sp2)···O distances are shorter by 0.3–0.5 Å; red shifts $\Delta\nu$C(sp2)H demonstrate a 5- to 8-fold increase; E_{HB} values, ∼10–12 kcal·mol^{-1}, more than double relative to the those of crystal (∼4–6 kcal·mol^{-1}). A similar strengthening is also found for the C(sp3)H···$[OAc]^-$ CAHBs in the gas phase (E_{HB} of ∼4–5 kcal·mol^{-1} depending on the empirical approach used) relative to those in the solid state (E_{HB} of ∼3–4 kcal·mol^{-1}). Moreover, the C7H···$[OAc]^-$ H-bond in isolated ion pairs is red-shifting instead of blue-shifting like in the crystal (Table 1). The range of $\Delta\nu$C7H is unprecedented for nonconventional H-bonds, that is, from −87 cm^{-1} in the gas to +36 cm^{-1} in the crystal. These dramatic changes in strengths and even in type of H-bonding are apparently caused by multiple secondary interactions functioning in the crystal and represented only on a much limited scale in the ion pairs discussed above.

The strengthening of nonconventional C(sp2)H···$[OAc]^-$ H-bonds in the gas phase implies that they have properties characteristic of strong conventional H-bonds where proton transfer is often observed. Moreover, as has been recently shown,[48−51] the acetate anion can be regarded as an "internal" deprotonating agent in imidazolium-based ionic liquids, where the imidazolium cation can be considered as a protonated N-heterocyclic carbene.[52−55] Notably, the acetate anion is able to deprotonate 1,3-dialkylimidazolium cations in the gas phase[48] to form carbenes. The formation of a H-bond between the C2H proton and the $[OAc]^-$ anion can be regarded as the first step in this process. The enthalpy of the (C2)H···$[OAc]^-$ hydrogen bond ($-\Delta H_{HB}$) for $[C_4mim][OAc]$ ion pair **7** (Figure 2), taken as a typical representative of 1,3-dialkylimidazolium acetates, amounts to 10 kcal·mol^{-1}. Despite such a strong H-bond, the (C2)H proton did not transfer to the anion. Moreover, attempts to optimize a carbene structure similar to **8** (Figure 2) were unsuccessful. The H-shifted structure **8** (Figure 2) was successfully optimized when one of two oxygen atoms of $[OAc]^-$ was freed from the short contact with the methylene group at the N1 atom (shown with the dotted line for ion pair **7** in Figure 2). Proton transfer from the cation to another oxygen atom of the anion (structure **8**) was found to be irreversible.

Similar to the case of $[C_4mim][OAc]$, H-shifted isomers of the ion pairs (structures **4**, **5** and **6** in Figure 2) were optimized only provided that one of the oxygen atoms of the anion was devoid of short contacts. Thus, the secondary interactions of the $[OAc]^-$ anion inhibit proton transfer from the $[C_4mim]^+$ and $[C_2OHmim]^+$ cations to the anion, whereas in their absence the protons of the imidazolium ring irreversibly shift to the acetate.

The most stable $[C_2OHmim][OAc]$ ion pair **1** (Figure 2) is stabilized by a strong OH···$[OAc]^-$ H-bond, which results in the high energy difference (ΔE) between this structure and the H-shifted isomer **4**. This ΔE value is larger by 10 kcal·mol^{-1} than ΔE^* in $[C_4mim][OAc]$ (Figure 2), which suggests that the formation of carbene species for $[C_2OHmim][OAc]$ is much less likely than that for nonfunctionalized 1,3-dialkylimidazolium acetates.

In summary, DFT computations of crystalline $[C_2OHmim][OAc]$ in combination with structural and spectroscopic studies have provided the first quantitative characteristics of the strength of conventional and nonconventional H-bonds formed by the acetyl anion in molecular crystals. Notably, a comparison of these data with the corresponding "gas-phase' values obtained quantum chemically, together with data reported earlier for related systems, revealed a markedly different behaviour of conventional OH···$[OAc]^-$ and nonconventional CH···$[OAc]^-$ H-bonds.

With CAHBs involving OH groups, the strength of OH···$[OAc]^-$ H-bonds is not particularly influenced by the phase state of the $[C_2OHmim][OAc]$ salt. Depending on the empirical approach used, E_{HB} estimates of 9–12 kcal·mol^{-1} for the crystal and 11–13 kcal·mol^{-1} for the gas phase were obtained. A moderate strengthening of ∼2 kcal·mol^{-1} was reported previously for much weaker OH···$[PF_6]^-$ H-bonds in isolated $[C_2OHmim][PF_6]$ ion pairs relative to the bulk ionic liquid.[28] Thus, gas-phase E_{HB} evaluations for CAHBs involving OH groups, irrespective of their strength, require only small corrections for condensed-phase systems.

Moreover, E_{HB} estimates for OH···$[A]^-$ H-bonds formed by the $[C_2OHmim]^+$ cation in neat $[C_2OHmim][A]$-type ionic liquids compare well with the strengths of the H-bonds formed by methanol with the same anions (A = PF_6^-, BF_4^-, and $CF_3SO_3^-$), both in "innocent" (CH_2Cl_2) and "non-innocent" ($[C_4mim][PF_6]$) solvents. The strengthening of the H-bonds relative to MeOH caused by the positive charge on the $[C_2OHmim]^+$ cation is <20% (Table 2). Thus, neither cooperativity nor positive-charge assistance play a significant role in the OH···$[A]^-$ H-bonding, and even neutral H-bond donors can serve as suitable models to quantify CAHBs formed by OH groups with different anions.

In contrast, nonconventional CH···$[A]^-$ CAHBs are almost as strong as OH···$[A]^-$ H-bonds in the gas phase but are weakened by ∼50% by cooperative effects in the condensed phase. This weakening could explain why the $[OAc]^-$ anion deprotonates the $[C_4mim]^+$ cation only in the gas[48] but not in the condensed phase.[56] These effects transform the C(sp3)H···$[OAc]^-$ H-bond from "proper" in the gas to "improper" in the crystal and even inactivate the ability of the $[OAc]^-$ anion to deprotonate the imidazolium cation, thus preventing carbene formation in neat ionic liquids.[57−59] Probably these differences in the behavior of OH···$[A]^-$ and CH···$[A]^-$ H-bonds could be

DOI: 10.1021/acs.jpclett.5b02175
J. Phys. Chem. Lett. 2015, 6, 4431−4436

explained by the different balance of covalent and electrostatic components in conventional and nonconventional H-bonds. The former component should be less susceptible to the influence of the surrounding media compared to the latter.

These findings suggest that the strengths of conventional OH···$[A]^-$ CAHBs in condensed phases can be deduced from the gas phase, whereas analysis of the role of nonconventional CH···$[A]^-$ CAHBs in the condensed phases based only on their gas-phase strength estimates can be misleading. Nevertheless, our present results imply that half of the gas-phase energy of an isolated CH···$[A]^-$ CAHB could be used as a reasonable approximation for the corresponding condensed-state value.

■ ASSOCIATED CONTENT

Supporting Information

The Supporting Information is available free of charge on the ACS Publications website at DOI: 10.1021/acs.jpclett.5b02175.

Crystal data from X-ray, assignment of IR bands in the spectrum of the solid $[C_2OHmim][OAc]$, and details of experiment and computations (PDF)

■ AUTHOR INFORMATION

Corresponding Authors

*E-mail: skatsyuba@yahoo.com or katsyuba@iopc.ru (S.A.K.).
*E-mail: paul.dyson@epfl.ch (P.J.D.).

Notes

The authors declare no competing financial interest.

■ ACKNOWLEDGMENTS

Financial support from the EPFL is gratefully acknowledged. M.V.V. and S.A.K. thank the Russian Foundation for Basic Research (Grants 14-03-01031 and 15-03-01058 A, respectively) for partial financial support of this study.

■ REFERENCES

(1) Meot-Ner, M. Update 1 of: Strong Ionic Hydrogen Bonds. *Chem. Rev.* **2012**, *112*, PR22−PR103.

(2) Gronert, S. Theoretical studies of proton transfers. 1. The Potential Energy Surfaces of the Identity Reactions of the First- and Second-row Non-Metal Hydrides with Their Conjugate Bases. *J. Am. Chem. Soc.* **1993**, *115*, 10258−10266.

(3) Kim, K. S.; Lee, J. Y.; Lee, S. J.; Ha, T.-K.; Kim, D. H. On Binding Forces between Aromatic Ring and Quaternary Ammonium Compound. *J. Am. Chem. Soc.* **1994**, *116*, 7399−7400.

(4) Raymo, F. M.; Bartberger, M. D.; Houk, K. N.; Stoddart, J. F. The Magnitude of [C−H···O] Hydrogen Bonding in Molecular and Supramolecular Assemblies. *J. Am. Chem. Soc.* **2001**, *123*, 9264−9267.

(5) Scheiner, S.; Kar, T.; Pattanayak, J. Comparison of Various Types of Hydrogen Bonds Involving Aromatic Amino Acids. *J. Am. Chem. Soc.* **2002**, *124*, 13257−13264.

(6) Cannizzaro, C. E.; Houk, K. N. Magnitudes and Chemical Consequences of R_3N^+−C−H···OC Hydrogen Bonding. *J. Am. Chem. Soc.* **2002**, *124*, 7163−7169.

(7) Bryantsev, V. S.; Hay, B. P. Are C−H Groups Significant Hydrogen Bonding Sites in Anion Receptors? Benzene Complexes with Cl^-, NO_3^-, and ClO_4^-. *J. Am. Chem. Soc.* **2005**, *127*, 8282−8283.

(8) Shishkin, O. V.; Palamarchuk, G. V.; Gorb, L.; Leszczynski, J. Opposite Charges Assisted Extra Strong C−H···O Hydrogen Bond in Protonated 2′-Deoxyadenosine Monophosphate. *Chem. Phys. Lett.* **2008**, *452*, 198−205.

(9) Gilli, P.; Pretto, L.; Bertolasi, V.; Gilli, G. Predicting Hydrogen-Bond Strengths from Acid−Base Molecular Properties. The pKa Slide Rule: Toward the Solution of a Long-Lasting Problem. *Acc. Chem. Res.* **2009**, *42*, 33−44.

(10) Nepal, B.; Scheiner, S. Anionic CH···X− Hydrogen Bonds: Origin of Their Strength, Geometry, and Other Properties. *Chem. - Eur. J.* **2015**, *21*, 1474−1481.

(11) Adhikari, U.; Scheiner, S. Magnitude and Mechanism of Charge Enhancement of CH··O Hydrogen Bonds. *J. Phys. Chem. A* **2013**, *117*, 10551−10562.

(12) Jeffrey, G. A.; Saenger, W. *Hydrogen bonding in biological structures*; Springer: Berlin, Germany, 1991.

(13) Scheiner, S. *Hydrogen Bonding. A Theoretical Perspective*; Oxford University Press: Oxford, U.K., 1997.

(14) Gilli, G.; Gilli, P. *The Nature of the Hydrogen Bond. Outline of a Comprehensive Hydrogen Bond Theory*; Oxford University Press: Oxford, U.K., 2009.

(15) Hosseini, M. W. Molecular Tectonics: from Molecular Recognition of Anions to Molecular Networks. *Coord. Chem. Rev.* **2003**, *240*, 157−166.

(16) Castellano, R. K. Progress Toward Understanding the Nature and Function of C-H···O Interactions. *Curr. Org. Chem.* **2004**, *8*, 845−865.

(17) Tatko, C. D.; Waters, M. L. Comparison of C−H···π and Hydrophobic Interactions in a β-Hairpin Peptide: Impact on Stability and Specificity. *J. Am. Chem. Soc.* **2004**, *126*, 2028−2034.

(18) Garczarek, F.; Brown, L. S.; Lanyi, J. K.; Gerwert, K. Proton Binding within a Membrane Protein by a Protonated Water Cluster. *Proc. Natl. Acad. Sci. U. S. A.* **2005**, *102*, 3633−3638.

(19) Babu, N. J.; Reddy, L. S.; Nangia, A. Amide−N-Oxide Heterosynthon and Amide Dimer Homosynthon in Cocrystals of Carboxamide Drugs and Pyridine N-Oxides. *Mol. Pharmaceutics* **2007**, *4*, 417−434.

(20) Schmiedekamp, A.; Nanda, V. Metal-Activated Histidine Carbon Donor Hydrogen Bonds Contribute to Metalloprotein Folding and Function. *J. Inorg. Biochem.* **2009**, *103*, 1054−1060.

(21) Sukumar, N.; Mathews, F. S.; Langan, P.; Davidson, V. L. A Joint X-ray and Neutron Study on Amicyanin Reveals the Role of Protein Dynamics in Electron Transfer. *Proc. Natl. Acad. Sci. U. S. A.* **2010**, *10*, 6817−6822.

(22) Kong, S.; Shenderovich, I. G.; Vener, M. V. Density Functional Study of the Proton Transfer Effect on Vibrations of Strong (Short) Intermolecular O−H···N/O−···H−N^+ Hydrogen Bonds in Aprotic Solvents. *J. Phys. Chem. A* **2010**, *114*, 2393−2399.

(23) Bondar, A.-N.; Dau, H. Extended Protein/Water H-bond Networks in Photosynthetic Water Oxidation. *Biochim. Biophys. Acta, Bioenerg.* **2012**, *1817*, 1177−1190.

(24) Maiorov, V. D.; Kislina, I. S.; Rykounov, A. A.; Vener, M. V. The Structure and Vibrational Features of Proton Disolvates in Water−Ethanol Solutions of HCl: the Combined Spectroscopic and Theoretical Study. *J. Phys. Org. Chem.* **2014**, *27*, 135−141.

(25) Bader, R. W. F. *Atoms in Molecules: A Quantum Theory*; Oxford University Press: New York, 1990.

(26) Mata, I.; Alkorta, I.; Espinosa, E.; Molins, E. Relationships between Interaction Energy, Intermolecular Distance and Electron Density Properties in Hydrogen Bonded Complexes under External Electric Fields. *Chem. Phys. Lett.* **2011**, *507*, 185−189.

(27) Nelyubina, Y. V.; Antipin, M. Y.; Lyssenko, K. A. Are Halide··· Halide Contacts a Feature of Rock-Salts Only? *J. Phys. Chem. A* **2007**, *111*, 1091−1095.

(28) Katsyuba, S. A.; Vener, M. V.; Zvereva, E. E.; Fei, Z.; Scopelliti, R.; Laurenczy, G.; Yan, N.; Paunescu, E.; Dyson, P. J. How Strong Is Hydrogen Bonding in Ionic Liquids? Combined X-ray Crystallographic, Infrared/Raman Spectroscopic, and Density Functional Theory Study. *J. Phys. Chem. B* **2013**, *117*, 9094−9105.

(29) Iogansen, A. V. Direct Proportionality of the Hydrogen Bonding Energy and the Intensification of the Stretching ν(XH) Vibration in Infrared Spectra. *Spectrochim. Acta, Part A* **1999**, *55*, 1585−1612.

(30) Purcell, K. F.; Drago, R. S. Theoretical Aspects of the Linear Enthalpy Wavenumber Shift Relation for Hydrogen-Bonded Phenols. *J. Am. Chem. Soc.* **1967**, *89*, 2874−2879.

(31) Bankiewicz, B.; Matczak, P.; Palusiak, M. Electron Density Characteristics in Bond Critical Point (QTAIM) versus Interaction

DOI: 10.1021/acs.jpclett.5b02175
J. Phys. Chem. Lett. 2015, 6, 4431−4436

Energy Components (SAPT): The Case of Charge-Assisted Hydrogen Bonding. *J. Phys. Chem. A* **2012**, *116*, 452−459.
(32) Anand, M.; Fernández, I.; Schaefer, H. F.; Wu, J. I. C. Hydrogen Bond−Aromaticity Cooperativity in Self-Assembling 4-Pyridone Chains. *J. Comput. Chem.* **2015**, DOI: 10.1002/jcc.23976.
(33) Alabugin, I. V.; Manoharan, M.; Peabody, S.; Weinhold, F. Electronic Basis of Improper Hydrogen Bonding: A Subtle Balance of Hyperconjugation and Rehybridization. *J. Am. Chem. Soc.* **2003**, *125*, 5973−5987.
(34) Bankiewicz, B.; Palusiak, M. Does Electron Density in Bond Critical Point Reflect the Formal Charge Distribution in H-Bridges? The Case of Charge-Assisted Hydrogen Bonds (CAHBs). *Comput. Theor. Chem.* **2011**, *966*, 113−119.
(35) Macchi, P.; Iversen, B. B.; Sironi, A.; Chakoumakos, B. C.; Larsen, F. K. Interanionic O−H···O Interactions: The Charge Density Point of View. *Angew. Chem., Int. Ed.* **2000**, *39*, 2719−2722.
(36) Beichel, W.; Trapp, N.; Hauf, C.; Kohler, O.; Eickerling, G.; Scherer, W.; Krossing, I. Charge-Scaling Effect in Ionic Liquids from the Charge-Density Analysis of N,N′-Dimethylimidazolium Methylsulfate. *Angew. Chem., Int. Ed.* **2014**, *53*, 3143−3146.
(37) Vener, M. V.; Egorova, A. N.; Churakov, A. V.; Tsirelson, V. G. Intermolecular Hydrogen Bond Energies in Crystals Evaluated Using Electron Density Properties: DFT Computations with Periodic Boundary Conditions. *J. Comput. Chem.* **2012**, *33*, 2303−2309.
(38) Shishkina, A. V.; Zhurov, V. V.; Stash, A. I.; Vener, M. V.; Pinkerton, A. A.; Tsirelson, V. G. Noncovalent Interactions in Crystalline Picolinic Acid N-Oxide: Insights from Experimental and Theoretical Charge Density Analysis. *Cryst. Growth Des.* **2013**, *13*, 816−828.
(39) Rozenberg, M.; Loewenschuss, A.; Marcus, Y. An Empirical Correlation between Stretching Vibration Redshift and Hydrogen Bond Length. *Phys. Chem. Chem. Phys.* **2000**, *2*, 2699−2702.
(40) The scaling factor value of 0.964 was obtained from comparison of B3LYP-D3/6-31G** computed νOH frequency of methanol (3824 cm^{-1}) with the corresponding experimental frequency of methanol in the gas phase (3687 cm^{-1}). The obtained value was used for scaling of the computed frequencies of OH and CH stretching vibrations of [C_2OHmim] cation.
(41) Scheiner, S. Identification of Spectroscopic Patterns of CH···O H-Bonds in Proteins. *J. Phys. Chem. B* **2009**, *113*, 10421−10427.
(42) Scheiner, S.; Kar, T. Spectroscopic and Structural Signature of the CH−O Hydrogen Bond. *J. Phys. Chem. A* **2008**, *112*, 11854−11860.
(43) Saha, S.; Rajput, L.; Joseph, S.; Mishra, M. K.; Ganguly, S.; Desiraju, G. R. IR Spectroscopy as a Probe for C-H··X hydrogen Bonded Supramolecular Synthons. *CrystEngComm* **2015**, *17*, 1273−1290.
(44) Vener, M. V.; Egorova, A. N.; Fomin, D. P.; Tsirelson, V. G. Hierarchy of the Non-Covalent Interactions in the Alanine-Based Secondary Structures. DFT Study of the Frequency Shifts and Electron-Density Features. *J. Phys. Org. Chem.* **2009**, *22*, 177−185.
(45) Hermansson, K. Blue-Shifting Hydrogen Bonds. *J. Phys. Chem. A* **2002**, *106*, 4695−4702.
(46) Cammarata, L.; Kazarian, S. G.; Salter, P. A.; Welton, T. Molecular States of Water in Room Temperature Ionic Liquids. *Phys. Chem. Chem. Phys.* **2001**, *3*, 5192−5200.
(47) Kristiansson, O.; Schuisky, M. Interaction between Methanol and the Cl^-, Br^-, I^-, NO_3^-, ClO_4^-, BF_4^-, $SO_3CF_3^-$ and PF_6^- Anions Studied by FTIR Spectroscopy. *Acta Chem. Scand.* **1997**, *51*, 270−273.
(48) Holloczki, O.; Gerhard, D.; Massone, K.; Szarvas, L.; Nemeth, B.; Veszpremi, T.; Nyulaszi, L. Carbenes in Ionic Liquids. *New J. Chem.* **2010**, *34*, 3004−3009.
(49) Rodriguez, H.; Gurau, G.; Holbrey, J. D.; Rogers, R. D. Reaction of Elemental Chalcogens with Imidazolium Acetates to Yield Imidazole-2-Chalcogenones: Direct Evidence for Ionic Liquids as Proto-Carbenes. *Chem. Commun.* **2011**, *47*, 3222−3224.
(50) Kelemen, Z.; Holloczki, O.; Nagy, J.; Nyulaszi, L. An Organocatalytic Ionic Liquid. *Org. Biomol. Chem.* **2011**, *9*, 5362−5364.
(51) Hollóczki, O.; Nyulászi, L. Carbenes from Ionic Liquids. In *Electronic Effects in Organic Chemistry*; Kirchner, B., Ed. Springer: Berlin, Heidelberg, Germany, 2014; Vol. *351*, pp 1−24.
(52) Schönherr, H.-J.; Wanzlick, H.-W. Chemie Nucleophiler Carbene, XVIII1) 1.3.4.5-Tetraphenyl-Imidazoliumperchlorat. *Liebigs Ann. Chem.* **1970**, *731*, 176−179.
(53) Melaimi, M.; Soleilhavoup, M.; Bertrand, G. Stable Cyclic Carbenes and Related Species beyond Diaminocarbenes. *Angew. Chem., Int. Ed.* **2010**, *49*, 8810−8849.
(54) Diez-Gonzalez, S. *N-heterocyclic Carbenes: From Laboratory Curiosities to Efficient Synthetic Tools*; Royal Society of Chemistry: Cambridge, U.K., 2011.
(55) Arduengo, A. J.; Bertrand, G. Carbenes Introduction. *Chem. Rev.* **2009**, *109*, 3209−3210.
(56) Holloczki, O.; Firaha, D. S.; Friedrich, J.; Brehm, M.; Cybik, R.; Wild, M.; Stark, A.; Kirchner, B. Carbene Formation in Ionic Liquids: Spontaneous, Induced, or Prohibited? *J. Phys. Chem. B* **2013**, *117*, 5898−907.
(57) Distillability of ionic liquids (ref 58) was ascribed either to evaporation of neutral ion pairs or to formation of free carbenes and acids by a proton transfer from the cation to the anion (ref 59). Our work suggests that the latter process can proceed only after evaporation, that is, in the gas phase.
(58) Earle, M. J.; Esperanca, J. M. S. S.; Gilea, M. A.; Canongia Lopes, J. N.; Rebelo, L. P. N.; Magee, J. W.; Seddon, K. R.; Widegren, J. A. The Distillation and Volatility of Ionic Liquids. *Nature* **2006**, *439*, 831−834.
(59) Malberg, F.; Brehm, M.; Holloczki, O.; Pensado, A. S.; Kirchner, B. Understanding the Evaporation of Ionic Liquids Using the Example of 1-Ethyl-3-Methylimidazolium Ethylsulfate. *Phys. Chem. Chem. Phys.* **2013**, *15*, 18424−18436.

DOI: 10.1021/acs.jpclett.5b02175
J. Phys. Chem. Lett. 2015, 6, 4431−4436